Journal of Visualized Experiments

A Modified Surgical Model of Hind Limb Ischemia in ApoE-/- Mice Using a Miniature Incision

--Manuscript Draft--

Article Type:	Methods Article - JoVE Produced Video
Manuscript Number:	JoVE62402R2
Full Title:	A Modified Surgical Model of Hind Limb Ischemia in ApoE-/- Mice Using a Miniature Incision
Corresponding Author:	Michael Keese Heidelberg University GERMANY
Corresponding Author's Institution:	Heidelberg University
Corresponding Author E-Mail:	Michael.keese@umm.de
Order of Authors:	Kaixuan Yan
	Jiaxing Zheng
	Frank Zöllner
	Kay Schwenke
	Prama Pallavi
	Michael Keese
Additional Information:	
Question	**Response**
Please indicate whether this article will be Standard Access or Open Access.	Standard Access (US$2,400)
Please specify the section of the submitted manuscript.	Medicine
Please indicate the **city, state/province, and country** where this article will be **filmed**. Please do not use abbreviations.	Mannheim, Germany
Please confirm that you have read and agree to the terms and conditions of the author license agreement that applies below:	I agree to the Author License Agreement
Please provide any comments to the journal here.	
Please indicate whether this article will be Standard Access or Open Access.	Standard Access ($1400)

TITLE:

A Modified Surgical Model of Hind Limb Ischemia in ApoE$^{-/-}$ Mice Using a Miniature Incision

AUTHORS AND AFFILIATIONS:

Kaixuan Yan[1,2] , Jiaxing Zheng[1,2] , Frank G. Zöllner[3,4] , Kay Schwenke[1] , Prama Pallavi[1,2] , Michael Keese[1,2]

[1]Department of Surgery, Medical Faculty Manheim, Mannheim University Medical Centre, University of Heidelberg, Mannheim, Germany

[2]European Center of Angioscience ECAS, Medical Faculty Mannheim of the University of Heidelberg, Mannheim, Germany

[3]Computer-Assisted Clinical Medicine, Mannheim Institute for Intelligent Systems in Medicine, Medical Faculty Mannheim, Heidelberg University, Mannheim, Germany

[4]Cooperative Core Facility Animal Scanner ZI, Medical Faculty Mannheim, Heidelberg University, Mannheim, Germany

E-mail addresses of co-authors:

Kaixuan Yan (Kaixuan.Yan@medma.uni-heidelberg.de)
Jiaxing Zheng (Jiaxing.Zheng@medma.uni-heidelberg.de)
Frank G. Zöllner (Frank.Zoellner@medma.uni-heidelberg.de)
Kay Schwenke (kay.schwenke@umm.de)
Prama Pallavi (Prama.pallavi@medma.uni-heidelberg.de)

***Corresponding author:**

Michael Keese (Michael.keese@umm.de)

KEYWORDS

hind limb ischemia model; mice; surgical approach; femoral artery, ApoE$^{-/-}$ mice

SUMMARY

This article demonstrates an efficient surgical approach to establish acute ischemia in mice with a small incision. This approach can be applied by most research groups without any laboratory upgrades.

ABSTRACT

The purpose of this study is to introduce and evaluate a modified surgical approach to induce acute ischemia in mice that can be implemented in most animal laboratories. Contrary to the conventional approach for double ligation of the femoral artery (DLFA), a smaller incision on the right inguinal region was made to expose the proximal femoral artery (FA) to perform DLFA. Then, using a 7-0 suture, the incision was dragged to the knee region to expose the distal FA. Magnetic resonance imaging (MRI) on bilateral hind limbs was used to detect FA blockage after the surgery. At 0, 1, 3, 5, and 7 days after the surgery, functional recovery of the hind limbs was visually assessed and graded using the Tarlov scale. Histologic evaluation was performed after euthanizing the animals 7 days after DLFA. The procedures were successfully performed on the

right leg in ten ApoE$^{-/-}$ mice, and no mice died during subsequent observation. The incision sizes in all 10 mice were all less than 5 mm (4.2 ± 0.63 mm). MRI results showed that FA blood flow in the ischemic side was clearly blocked. The Tarlov scale results demonstrated that hind limb function significantly decreased after the procedure and slowly recovered over the following 7 days. Histologic evaluation showed a significant inflammatory response on the ischemic side and reduced microvascular density in the ischemic hind limb. In conclusion, this study introduces a modified technique using a miniature incision to perform hind limb ischemia (HLI) using DLFA.

INTRODUCTION:

There is an unmet need for preclinical animal models for research in vascular diseases such as peripheral artery disease (PAD). Despite the advanced developments in diagnosis and treatment, there were more than 200 million patients with PAD in 2018[1], and their number is constantly increasing. Although several novel therapeutic approaches[2-7] have been described, successful translation of these therapeutic modalities into clinical application remains a daunting task. Therefore, reliable and relevant *in vivo* experimental models simulating the human disease condition are required to investigate the potential mechanism and efficiency of these new therapeutic approaches to treat PAD[6,7].

Hyperlipidemia and atherosclerosis (AS) are the main risk factors for the development of PAD. ApoE$^{-/-}$ mice (on a high-fat diet) display abnormal fat metabolism and hyperlipidemia and subsequently develop atherosclerotic plaques rendering ApoE$^{-/-}$ mice as the best choice to simulate the clinically relevant PAD. Preclinical HLI animal models are generated through double ligation of the femoral artery (DLFA), which is the most widely used approach in laboratories all over the world[8-15] to simulate acute-on-chronic ischemia. However, this approach usually requires a relatively large and invasive incision. Furthermore, it inevitably leads to the animals (especially mice) suffering from increased pain injury and inflammation, which also influences the subsequent experimental results[5,6,16,17]. This paper describes an acute-on-chronic HLI model in APOE$^{-/-}$ mice by using a very small incision.

PROTOCOL:

NOTE: All experimental procedures were approved by the University Committee on animal care of Heidelberg University (G-239/18) and were performed according to the NIH guideline for the care and use of laboratory animals. Ten male ApoE$^{-/-}$ mice with the C57BL/6J background, weighing 29.6–38.0 g, were housed on a 12 h light/dark cycle and fed a western diet (1.25% cholesterol and 21% fat) and water *ad libitum* for 12 weeks from the age of 8 weeks. HLI was performed on 20-week-old mice as described below.

1. Induction of HLI in ApoE$^{-/-}$ mice

1.1. Prepare the required equipment and tools for surgery (see the **Table of Materials** and **Figure 1**).

1.2. Anesthetize the mouse with a subcutaneous injection (S.C.) of a mixture of midazolam (5

mg/kg), medetomidine (0.05 mg/ml/kg), and fentanyl (0.5 mg/kg) before all surgical procedures.

1.2.1. After onset of anesthesia, use the vet ointment on the eyes to prevent dryness, and confirm the absence of the pedal withdrawal reflex in the forelimb and hind limb.

1.3. Afterwards place the mouse on a heating pad to keep the core body temperature at approximately 37 °C. Using cotton swab and hair removal cream, carefully remove hair from the hind limb skin on the right side.

1.4. Lay the mouse in the supine position on the heating pad under a dissecting microscope. Use alcohol wipes to clean the skin of the mouse. Afterwards, use pointed forceps and surgical scissors to make an approximately 3–4 mm incision in the middle of the inguinal region. See **Figure 2** for a schematic of the procedure.

1.5. Remove the subcutaneous fat tissue carefully with help of fine pointed forceps to expose the proximal femoral neurovascular bundle. Carefully use the fine pointed forceps to pierce the membrane of the femoral sheath. Use a cotton swab moistened with saline to move the femoral artery (FA) carefully away from the femoral nerve (FN) and femoral vein (FV).

1.6. Pass two 7-0 absorbable sutures through the proximal FA, and make double knots using spring scissors to transect the FA between the two ties.

1.7. To expose the distal FA, pass a 7-0 absorbable suture through the lower edge of the incision and gently drag the incision to the region of the right side of the knee of the hind limb.

1.8. Move the subcutaneous tissue aside carefully to expose the neurovascular bundle. Use fine pointed forceps to pierce the membrane of the femoral sheath, and dissect the FA from the FV and FN.

1.9. Pass two 7-0 absorbable sutures through the distal FA, and make double knots. Use spring scissors to transect the FA between the two ties.

NOTE: No ligation was performed on the left limb, which served as a control in each mouse.

1.10. Afterwards, use 6-0 absorbable sutures to stitch the incision. Place the mouse on a heating pad in a clean cage, and continue to monitor its breathing and heartbeat until it fully recovers.

2. Magnetic resonance imaging

NOTE: One day after DLFA, the mice must undergo MRI scans to assess FA blockage.

2.1. Place the mouse in a transparent induction chamber, and anesthetize the mouse with 1.5–2% isoflurane in ambient air until loss of righting reflex.

2.2. Place the mouse on a heated animal bed equipped with a bite holder and positioned toward the magnet with a laser-controlled system. Maintain the body temperature at 37 ± 1 °C.

2.3. During image acquisition, maintain anesthesia with 1.5–2% isoflurane in ambient air, and monitor the respiration using a pressure probe.

2.4. Acquire images in the transverse slice orientation using a three-dimensional (3D) time of flight (TOF) angiography sequence with parameter echo time (TE)/repetition time (TR)/flip angle (FA) = 2 ms/12 ms/13°, four averages, an acquisition matrix of 178 x 144 reconstructed to 256 x 192 and 121 slices, resulting in an isotropic resolution of 0.15 mm^3. To suppress the signal from the veins, place a saturation slice distally to the hind limbs.

3. Clinical evaluation and follow-up

3.1. Estimate the functional recovery in the 1^{st}, 3^{rd}, 5^{th}, and 7^{th} days after the surgery by using the functional scoring Tarlov scale[18,19] (**Table 1**).

4. Histologic evaluation

4.1. Seven days after the surgery, apply pentobarbital injection (115 mg/kg) to euthanize the mice.

4.2. Perfuse phosphate-buffered saline (PBS) containing 1% paraformaldehyde (PFA) through the left cardiac ventricle (100 mL per mouse). Fix the bilateral gastrocnemius (Gm) of the mice in 4% PFA overnight at 4 °C.

4.3. Embed the sample in paraffin according to the previously described protocol[20].

4.3.1. Cut 4–5-µm-thick sections of the paraffin-embedded tissue block on a microtome. With the help of a round paint brush, place the cut tissue sections in the water bath maintained at 42°C.

4.3.2. Insert the microscope slide into the water at a 45° angle, and carefully position it underneath the group of sections to be collected.

4.3.3. Carefully lift the slide from the water, and allow the sections to attach to the slide and dry overnight on the benchtop incubator at 37 °C.

4.4. Perform hematoxylin/eosin (HE) staining of the paraffin sections.

4.4.1. Place the slides containing the sections in slide holders. Prepare 3 containers of fresh xylene, and place the slides in each container for 5 min to deparaffinize the sections.

4.4.2. Rehydrate the sections by dipping the slices successively in 96%, 80%, 70%, 50%, 30% ethanol, and deionized water for 5 min each.

4.4.3. Stain in hematoxylin solution for 10 min.

4.4.4. Transfer the slices to a container of deionized water and rinse by placing under running tap water for 5 min.

4.4.5. Using a microscope, check the intensity of hematoxylin staining. If the staining enables identification of the cell nuclei clearly, continue to the next step. If the staining intensity does not facilitate identification of cell nuclei or if the intensity of staining is faint, place the slide in the hematoxylin solution for 1 min, repeat the washing with water (step 4.4.4), and then check again.

4.4.6. Counterstain in eosin-Y solution for 5 min.

4.4.7. Dehydrate the sections by dipping the slices successively into containers containing deionized water and 30%, 50%, 70%, 80%, and 96% ethanol successively for a duration 10 s each. Next, place the sections sequentially in three containers of fresh xylene for 10 s each.

4.4.8. Place the slides horizontally on microscopic slide storage maps with the sections facing upwards. Add enough mounting medium on the slide, and mount the slides with coverslips.

4.5. Perform the immunohistochemical (IHC) staining of the paraffin sections.

4.5.1. Repeat deparaffinization and rehydration steps 4.4.1–4.4.2. Then, immerse the sections in a container with 10 mM sodium citrate buffer, pH 6, and bring the sample to a boil in a microwave.

NOTE: As over- or under-heating of samples can cause inconsistent staining, maintain the temperature at just below the boiling point for 10 min.

4.5.2. Next, cool the sections on a benchtop for 30 min. Thereafter, wash the sections in PBS three times for 5 min. Carefully dry the area around the sample, and draw a large circle around the sample using a hydrophobic pen. .

NOTE: Never touch the sample. Marking with a hydrophobic pen creates a hydrophobic boundary, which facilitates the use of a smaller volume of antibody solution.

4.5.3. Quench endogenous peroxidase activity by placing the section in 0.3% H_2O_2 in PBS for 10 min. Block sections with 400 µL of block buffer (PBS contain 3% bovine serum albumin and 0.3% of non-ionic detergent) for 1 h at room temperature in a humidified chamber.

4.5.4. Wash the sections in PBS for 5 min. Next, add 100–400 µL of diluted anti-CD31 antibody (1:250) enough to cover the section. Following this, incubate sections overnight at 4 °C in a

humidified chamber.

NOTE: Ensure that the section is completely covered with the antibody solution.

4.5.5. Remove the primary antibody, and wash the sections thrice in PBS for a duration of 5 min each.

4.5.6. Prepare the 3, 3'-diaminobenzidine (DAB) mixture by adding 1 drop of the DAB concentrate to 1 mL of the DAB diluent, and mix well. Afterwards, add 100–400 µL of DAB mixture to the sections, and monitor closely by eye for 2 min until an acceptable staining intensity is observed.

NOTE: Ensure that the section is completely covered with the DAB mixture.

4.5.7. Afterwards, rinse under running tap water for 5 min. Perform hematoxylin staining as described in steps 4.4.3–4.4.5.

4.5.8. Perform eosin-Y staining described in step 4.4.6. Perform dehydration steps described in step 4.4.7.

4.5.9. Mounted the sections with coverslips by using mounting medium. Use ImageJ to estimate the percent of CD31 positive area (%) in 5 randomly selected fields (40x) that can be regarded as microvascular density as previously described[21].

5. Statistical analysis

5.1. Use statistical analysis software to express the results as mean ± standard deviation and to perform unpaired *t*-test on the comparisons. Consider $P < 0.05$ to be statistically significant.

REPRESENTATIVE RESULTS:

Characteristics of ApoE$^{-/-}$ mice

DLFA surgeries were successfully performed on 10 mice to establish the HLI model, and none of the mice died after the procedure. To follow changes in body weight, mice were weighed before the DLFA procedure (Pre-DLFA) and 7 days after the DLFA surgery (Post-DLFA). Pre-DLFA weights ranged from 29.6 to 38.0 g (mean 34.74 ± 2.47 g), and post-DLFA weights ranged from 26.5 to 34.1 g (mean 30.77 ± 2.15 g), which were significantly lower than the pre-DLFA weights ($P < 0.05$, **Figure 3A**). The time for the surgery ranged from 15 to 47 min (mean 34.2 ± 8.82 min, not including the anesthesia time). The incision size in 10 mice ranged from 3 to 5 mm (mean 4.2 ± 0.63 mm).

MRI scan and functional recovery

The MRI scans very clearly indicated that the proximal and distal regions of the right FA showed no perfusion (**Figure 3C**), indicating the success of this method. One day after the surgery, the

Tarlov Scale results were significantly decreased ($P < 0.05$). Although the results slowly increased over the following days, they were still lower than baseline until day 7 ($P < 0.05$, **Figure 3B**). These trends are consistent with previous reports[20]. No necrosis or gangrenous tissue development were observed in the bilateral sides of the hind limbs of any mice. However, the paws of the ischemic hind limbs in 7 mice were unable to stretch naturally compared to the contralateral side. In addition, paws of the ischemic hind limbs in 4 mice exhibited slight discoloration compared to the contralateral side (**Figure 3D**).

Histological analysis

In HE staining of the right Gm muscle, myofibers exhibited irregular ischemic necrosis. Proliferating satellite cells had replaced the necrotic myofibers and were distributed in a mass and/or with irregular dispersion. Myofibers exhibited inflammatory infiltration by multinucleated macrophages. Myofibers in the inflammatory regions had lost their normal morphological characteristics, and there were few regenerated myofibers. Transverse sections of these regenerated myofibers were round, the cytoplasm was stained red, and one small nucleus or multiple nuclei were located at the center. In contrast, this kind of inflammatory pattern was not observed in the left Gm (**Figure 4**). CD31 antibody staining was performed to identify endothelial cells of the vessel in the Gm samples, and ImageJ was used to evaluate the CD31-positive area—a surrogate for microvascular density—in each of five fields of view (40x) for each sample. Ischemic hind limbs exhibited significantly more microvascular density than the non-ischemic side ($P < 0.05$, **Figure 5**).

FIGURE AND TABLE LEGENDS:

Figure 1: Equipment and tools required for the experiment. (**A**) Dissecting microscope and heating pad required for the surgery. (**B**) Surgical tools: 1. 7-0 and 6-0 absorbable sutures, 2. needle holder, 3. toothless forceps, 4. spring scissors, 5. fine pointed forceps, 6. pointed forceps, and 7. surgical scissors.

Figure 2: Schematic illustration of the procedure. (**A** and **D**) A small incision is made on the inguinal region to expose the proximal femoral A, which is ligated. (**B** and **E**) A 6-0 suture is used to drag the incision to the knee region to expose the distal Femoral A, which is ligated. (**C**, **F**, and **G**) Stitching of the incision. Abbreviations: Femoral A = femoral artery; Femoral N = femoral nerve; Femoral V = femoral vein.

Figure 3: Characteristics of the PAD mouse model. (**A**) Comparison of the body weight before and 7 days after DLFA. (**B**) Functional recovery evaluated by the Tarlov Scale. (**C**) Magnetic resonance angiography indicates the proximal and distal FA in the left hind limb (white arrow), and on the right side, the proximal and distal FA disappear. (**D**) Changes in the appearance of the bilateral hind limb of mice No. 2 and No. 4, 1 and 7 days after DLFA. Values shown are mean ± standard deviation. *$P < 0.05$, ** $P < 0.001$, *** $P < 0.0001$, **** $P < 0.00001$; unpaired *t*-test. Abbreviations: PAD = peripheral artery disease; DLFA = double ligation of the femoral artery; FA = femoral artery; L = left; R = right.

Figure 4: HE staining of the gastrocnemius muscle. (**A**) Low-magnification image showing HE staining of the right Gm 7 days after the DLFA procedure. Inflammation was observed in the right Gm. (**B**) In the right Gm, necrotic myofibers exhibited inflammatory infiltration by macrophages (white arrow). The muscle fibers lose their normal morphological characteristics. There were very few regenerated myofibers (black arrow). (**C**) HE staining of normal myofibers of the right Gm. (**D**) The contralateral/left Gm (nonischemic) muscle shows a normal histologic pattern. Scale bars: A = 200 µm, B–D = 50 µm. Abbreviations: HE = hematoxylin-eosin; DLFA = double ligation of the femoral artery; Gm = gastrocnemius; L = left; R= right.

Figure 5: Comparison of the microvascular density of bilateral gastrocnemius muscle. (**A**) CD31-IHC staining of right Gm section (black arrows). (**B**) CD31-IHC staining of left Gm section (black arrows). (**C**) Quantification of the microvascular density of the right side, which was much less than that on the left side. Values shown are mean ± standard deviation. **** $P < 0.00001$; unpaired *t*-test. Scale bars: A, B = 20 µm. Abbreviations: CD31 = cluster of differentiation 31; IHC = immunohistochemical; Gm = gastrocnemius.

Table 1: Functional Scoring.

Supplemental Table S1: Summary of 25 papers from the current literature on the establishment of the PAD model.

DISCUSSION:

This study reports a modified, simplified, and surgically efficient approach to establish an HLI model in ApoE$^{-/-}$ mice using double ligation in the proximal and distal regions of the FA through a 3–4 mm incision without any required laboratory upgrades. The main characteristic of this method is the smaller size of the incision compared to previously reported studies describing mouse HLI models[8-12,15,20,22-24] .

Historically, an incision has been made from the knee to the media tight, inguinal, or even the abdomen for better exposure, ranging from 0.5 to 2 cm or more[9,11,15,19,22,25,26] (summarized in **Supplemental Table S1**). This paper describes a surgical technique to achieve DLFA and as a result, HLI, in mice with an incision < 5 mm (4.2 ± 0.63 mm). The FA was ligated before it branches into the popliteal artery and saphenous artery, causing ischemia in several muscle groups in the hind limb and resulting in moderate stress in mice. Although mice recovered functionally by 7th day post-operation (Tarlov score day before operation 6 ± 0, 1st day after the operation 3.9 ± 0.99 vs 7th day after the operation 5.2 ± 0.92), ischemic damage was observed in Gm at the histological level. First, Gm in the ischemic leg myofibers exhibited irregular ischemic necrosis and were infiltrated by multinucleated macrophages, similar to what has been reported in PAD patients[27,28]. Despite myofiber atrophy, a few regenerated myofibers were also observed, which is in line to a previous report[29].

Second, the microvascular density in the ischemic Gm on the 7th day after ligation was higher than in the non-ischemic leg, which has also been reported by Ministro et al.[30]. The recent focus in PAD therapy is not just limited to increase microvascular density compared to the non-ischemic

side, but also on the restoration of ischemia-induced loss of viable muscle tissue, which supports new vessel formation by providing a matrix of growth factors and biomechanical support[31]. Thus, this model also gives a wide window to test the effectiveness of new therapies with these foci. Furthermore, achieving HLI with smaller incision fits with the 3R concept of animal experimentation as a refinement of the surgical procedure, i.e., the small skin incisional size decreases the trauma and postoperative pain.

An ideal animal model also provides a relatively long therapeutic window. Various surgical procedures for establishing ischemia in mice have been reported and applied, and they exert different effects on blood flow restoration[21]. For induction of HLI, surgical methods normally focus on the iliac artery[12,19,23,32], femoral artery[24,33,34], and their branches[11,35], some including the femoral vein as well[36,37]. As the level of vascular ligation has no effect on blood flow restoration, the deciding factor is the extent of injury in the vascular tree[21]. For a single ligation of the femoral or iliac artery, a small incision is made in the inguinal or abdominal region, while the other branch interactions are still maintained, and the perfusion restoration in the mouse hind limb recovers completely within 7 days[21,38]. Thus, a single ligation is not sufficient in terms of providing a suitable therapeutic window to test the effects of different treatments. If branches from the FA also need to be ligated, the skin incision must be made even larger, which lengthens the surgical time. Therefore, HLI by DLFA in mouse offers a suitable therapeutic window in which the improvements induced by therapy can be efficiently monitored[9,21,22,25].

Establishing a clinically relevant HLI animal model is important to test the efficiency of novel therapeutic approaches, i.e., cell, stem cell, or gene therapy for PAD[2-4]. Several PAD models have been developed in mice[15,21], rats[39], and rabbits[40,41]. Del Giudice and colleagues established a rabbit hindlimb ischemia model created by percutaneous, transauricular, distal femoral artery embolization with calibrated particles that may overcome some of the limitations of existing animal models[40]. Liddell et al.[41] also created a rabbit PAD model by coiling the superficial FA through an endovascular approach, resulting in reduced hind limb reperfusion. Although larger animals, such as rabbits, may yield more convincing results[40,41], thus taking the therapies a step closer to clinical application, they require increased cost and time to obtain results.

Despite the heterogeneous risk profile of most patients with PAD, including hereditary and behavioral factors[42], ApoE$^{-/-}$ mice exhibit abnormal fat metabolism and hyperlipidemia symptoms, such as total cholesterol, triglycerides, very-low-density lipoprotein, and intermediate-density lipoprotein, replicating some of the main characteristics observed in patients with PAD. Furthermore, with the high-fat diet, these indicators significantly increase. Lo Sasso et al. reported that in these mice, arterial fat accumulation occurs at 3 months of age[43],and that an increase in AS lesions occurs with advancing age[43]. Thus, ApoE$^{-/-}$ mice are particularly well-suited for the acute-on-chronic ischemia-PAD model because they recapitulate the hypercholesterolemia commonly present in patients with PAD and provide a suitable platform to evaluate various therapies targeted at promoting neovascularization of ischemic limbs. Furthermore, the price–performance ratio of testing novel therapies with ApoE$^{-/-}$ mice is unbeatable.

Despite the advantages mentioned in the above paragraphs, there are two limitations to this model. First, mastering this method requires the experimenter to have sufficient microsurgical experience and familiarity with the anatomy of the mouse hind limb. Second, the limited surgical exposure and the amount of subcutaneous fat tissue in the hind limb of $ApoE^{-/-}$ mice increase the surgical difficulty. Therefore, some related practice is required for successful implementation of this technique. In conclusion, this study reports a modified and easy-to-implement, surgically efficient approach for establishing an HLI model in $ApoE^{-/-}$ mice using a small incision. The small incision significantly reduces trauma to the animal and can be applied by most research groups without any laboratory upgrades.

ACKNOWLEDGMENTS:

Authors thank Viktoria Skude, Alexander Schlund, and Felix Hörner for the excellent technical support.

DISCLOSURES:

The authors declare that the article content was composed in the absence of any commercial or financial relationships that could be construed as a potential conflict of interest.

REFERENCES:

1 Shu, J., Santulli, G. Update on peripheral artery disease: Epidemiology and evidence-based facts. *Atherosclerosis.* **275**, 379–381 (2018).

2 Tateishi-Yuyama, E. et al. Therapeutic angiogenesis for patients with limb ischaemia by autologous transplantation of bone-marrow cells: a pilot study and a randomised controlled trial. *Lancet.* **360** (9331), 427–435 (2002).

3 Wang, Z. X. et al. Efficacy of autologous bone marrow mononuclear cell therapy in patients with peripheral arterial disease. *Journal of Atherosclerosis and Thrombosis.* **21** (11), 1183–1196 (2014).

4 Botham, C. M., Bennett, W. L., Cooke, J. P. Clinical trials of adult stem cell therapy for peripheral artery disease. *Methodist Debakey Cardiovascular Journal.* **9** (4), 201–205 (2013).

5 van Weel, V. et al. Vascular endothelial growth factor overexpression in ischemic skeletal muscle enhances myoglobin expression in vivo. *Circulation Research.* **95** (1), 58–66 (2004).

6 Olea, F. D. et al. Vascular endothelial growth factor overexpression does not enhance adipose stromal cell-induced protection on muscle damage in critical limb ischemia. *Arteriosclerosis, Thrombosis, and Vascular Biology.* **35** (1), 184–188 (2015).

7 Peeters Weem, S. M. O., Teraa, M., de Borst, G. J., Verhaar, M. C., Moll, F. L. Bone marrow derived cell therapy in critical limb ischemia: a meta-analysis of randomized placebo controlled trials. *European Journal of Vascular and Endovascular Surgery.* **50** (6), 775–783 (2015).

8 Crawford, R. S. et al. Divergent systemic and local inflammatory response to hind limb demand ischemia in wild-type and ApoE-/- mice. *Journal of Surgical Research.* **183** (2), 952–962 (2013).

9 Niiyama, H., Huang, N. F., Rollins, M. D., Cooke, J. P. Murine model of hindlimb ischemia. *Journal of Visualized Experiments: JoVE.* (23), 1035 (2009).

10 Brenes, R. A. et al. Toward a mouse model of hind limb ischemia to test therapeutic angiogenesis. *Journal of Vascular Surgery.* **56** (6), 1669–1679; discussion 1679 (2012).

11 Peck, M. A. et al. A functional murine model of hindlimb demand ischemia. *Annals of Vascular Surgery.* **24** (4), 532–537 (2010).
12 Lejay, A. et al. A new murine model of sustainable and durable chronic critical limb ischemia fairly mimicking human pathology. *European Journal of Vascular and Endovascular Surgery.* **49** (2), 205–212 (2015).
13 Nagase, H., Yao, S., Ikeda, S. Acute and chronic effects of exercise on mRNA expression in the skeletal muscle of two mouse models of peripheral artery disease. *PLoS One.* **12** (8), e0182456 (2017).
14 Fu, J. et al. Hydrogen molecules (H2) improve perfusion recovery via antioxidant effects in experimental peripheral arterial disease. *Molecular Medicine Reports.* **18** (6), 5009–5015 (2018).
15 Yu, J., Dardik, A. A murine model of hind limb ischemia to study angiogenesis and arteriogenesis. *Methods in Molecular Biology.* **1717**, 135–143 (2018).
16 Pu, L. Q. et al. Enhanced revascularization of the ischemic limb by angiogenic therapy. *Circulation.* **88** (1), 208–215 (1993).
17 Takeshita, S. et al. Therapeutic angiogenesis. A single intraarterial bolus of vascular endothelial growth factor augments revascularization in a rabbit ischemic hind limb model. *Journal of Clinical Investigation.* **93** (2), 662–670 (1994).
18 Tarlov, I. M. Spinal cord compression studies. III. Time limits for recovery after gradual compression in dogs. *AMA Archives of Neurology and Psychiatry.* **71** (5), 588–597 (1954).
19 Westvik, T. S. et al. Limb ischemia after iliac ligation in aged mice stimulates angiogenesis without arteriogenesis. *Journal of Vascular Surgery.* **49** (2), 464–473 (2009).
20 Hellingman, A. A. et al. Variations in surgical procedures for hind limb ischaemia mouse models result in differences in collateral formation. *European Journal of Vascular and Endovascular Surgery.* **40** (6), 796–803 (2010).
21 Liu, Q. et al. CRISPR/Cas9‐mediated hypoxia inducible factor‐1α knockout enhances the antitumor effect of transarterial embolization in hepatocellular carcinoma. *Oncology Reports.* **40** (5), 2547–2557 (2018).
22 Padgett, M. E., McCord, T. J., McClung, J. M., Kontos, C. D. Methods for acute and subacute murine hindlimb ischemia. *Journal of Visualized Experiments: JoVE.* (112), 54166 (2016).
23 Pellegrin, M. et al. Experimental peripheral arterial disease: new insights into muscle glucose uptake, macrophage, and T-cell polarization during early and late stages. *Physiological Reports.* **2** (2), e00234 (2014).
24 Sun, Z. et al. VEGF-loaded graphene oxide as theranostics for multi-modality imaging-monitored targeting therapeutic angiogenesis of ischemic muscle. *Nanoscale.* **5** (15), 6857–6866 (2013).
25 Craige, S. M. et al. NADPH oxidase 4 promotes endothelial angiogenesis through endothelial nitric oxide synthase activation. *Circulation.* **124** (6), 731–740 (2011).
26 Kant, S. et al. Neural JNK3 regulates blood flow recovery after hindlimb ischemia in mice via an Egr1/Creb1 axis. *Nature Communications.* **10** (1), 4223 (2019).
27 Chevalier, J. et al. Obstruction of small arterioles in patients with critical limb ischemia due to partial endothelial-to-mesenchymal transition. *iScience.* **23** (6), 101251 (2020).
28 Kosmac, K. et al. Correlations of calf muscle macrophage content with muscle properties and walking performance in peripheral artery disease. *Journal of the American Heart Association.*

9 (10), e015929 (2020).
29 Mohiuddin, M. et al. Critical limb ischemia induces remodeling of skeletal muscle motor unit, myonuclear-, and mitochondrial-domains. *Scientific Reports.* **9** (1), 9551 (2019).
30 Ministro, A. et al. Assessing therapeutic angiogenesis in a murine model of hindlimb ischemia. *Journal of Visualized Experiments: JoVE.* (148), e59582 (2019).
31 Kilarski, W. W., Samolov, B., Petersson, L., Kvanta, A., Gerwins, P. Biomechanical regulation of blood vessel growth during tissue vascularization. *Nature Medicine.* **15** (6), 657–664 (2009).
32 Portou, M. J. et al. Hyperglycaemia and ischaemia impair wound healing via Toll-like receptor 4 pathway activation in vitro and in an experimental murine model. *European Journal of Vascular and Endovascular Surgery.* **59** (1), 117–127 (2020).
33 Dokun, A. O. et al. A quantitative trait locus (LSq-1) on mouse chromosome 7 is linked to the absence of tissue loss after surgical hindlimb ischemia. *Circulation.* **117** (9), 1207–1215 (2008).
34 Hazarika, S. et al. MicroRNA-93 controls perfusion recovery after hindlimb ischemia by modulating expression of multiple genes in the cell cycle pathway. *Circulation.* **127** (17), 1818–1828 (2013).
35 Fan, W. et al. mTORC1 and mTORC2 play different roles in the functional survival of transplanted adipose-derived stromal cells in hind limb ischemic mice via regulating inflammation in vivo. *Stem Cells.* **31** (1), 203–214 (2013).
36 Terry, T. et al. CD34(+)/M-cadherin(+) bone marrow progenitor cells promote arteriogenesis in ischemic hindlimbs of ApoE(-)/(-) mice. *PLoS One.* **6** (6), e20673 (2011).
37 Kwee, B. J. et al. Treating ischemia via recruitment of antigen-specific T cells. *Science Advances.* **5** (7), eaav6313 (2019).
38 Nakada, M. T. et al. Clot lysis in a primate model of peripheral arterial occlusive disease with use of systemic or intraarterial reteplase: addition of abciximab results in improved vessel reperfusion. *Journal of Vascular and Interventional Radiology: JVIR.* **15** (2 Pt 1), 169–176 (2004)
39 Carr, A. N. et al. Efficacy of systemic administration of SDF-1 in a model of vascular insufficiency: support for an endothelium-dependent mechanism. *Cardiovascular Research.* **69** (4), 925–935 (2006).
40 Del Giudice, C. et al. Evaluation of a new model of hind limb ischemia in rabbits. *Journal of Vascular Surgery.* **68** (3), 849–857 (2018).
41 Liddell, R. P. et al. Endovascular model of rabbit hindlimb ischemia: a platform to evaluate therapeutic angiogenesis. *Journal of Vascular and Interventional Radiology: JVIR.* **16** (7), 991–998 (2005).
42 Aboyans, V. et al. 2017 ESC guidelines on the diagnosis and treatment of peripheral arterial diseases, in collaboration with the European Society for Vascular Surgery (ESVS): Document covering atherosclerotic disease of extracranial carotid and vertebral, mesenteric, renal, upper and lower extremity arteriesEndorsed by: the European Stroke Organization (ESO)The Task Force for the Diagnosis and Treatment of Peripheral Arterial Diseases of the European Society of Cardiology (ESC) and of the European Society for Vascular Surgery (ESVS). *European Heart Journal*. **39** (9), 763–816 (2018).
43 Lo Sasso, G. et al. The Apoe(-/-) mouse model: a suitable model to study cardiovascular and respiratory diseases in the context of cigarette smoke exposure and harm reduction. *Journal*

of Translational Medicine. **14** (1), 146 (2016).

Figure-1

Click here to access/download;Figure;Figure 1-revision.tiff

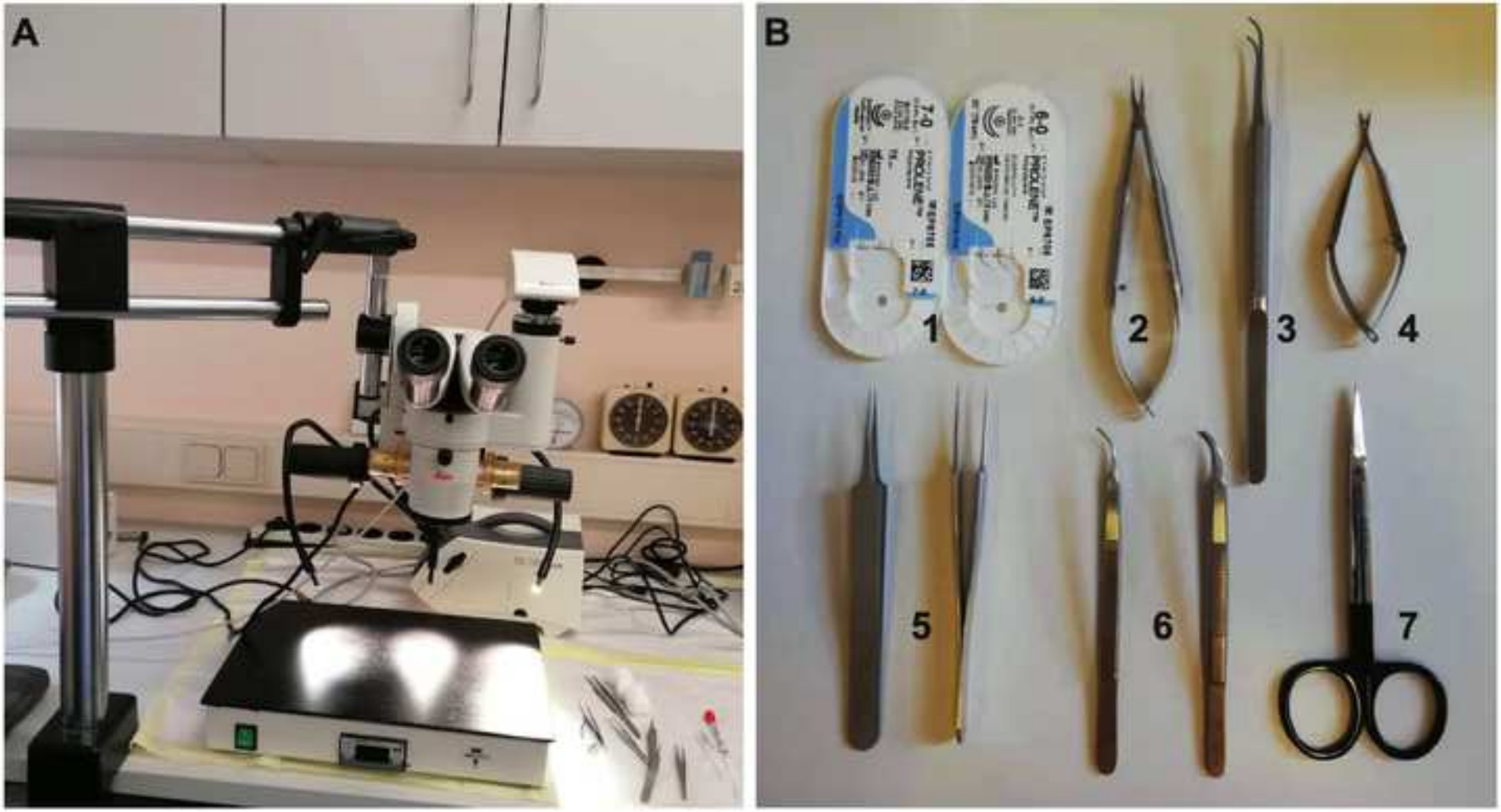

Figure-2

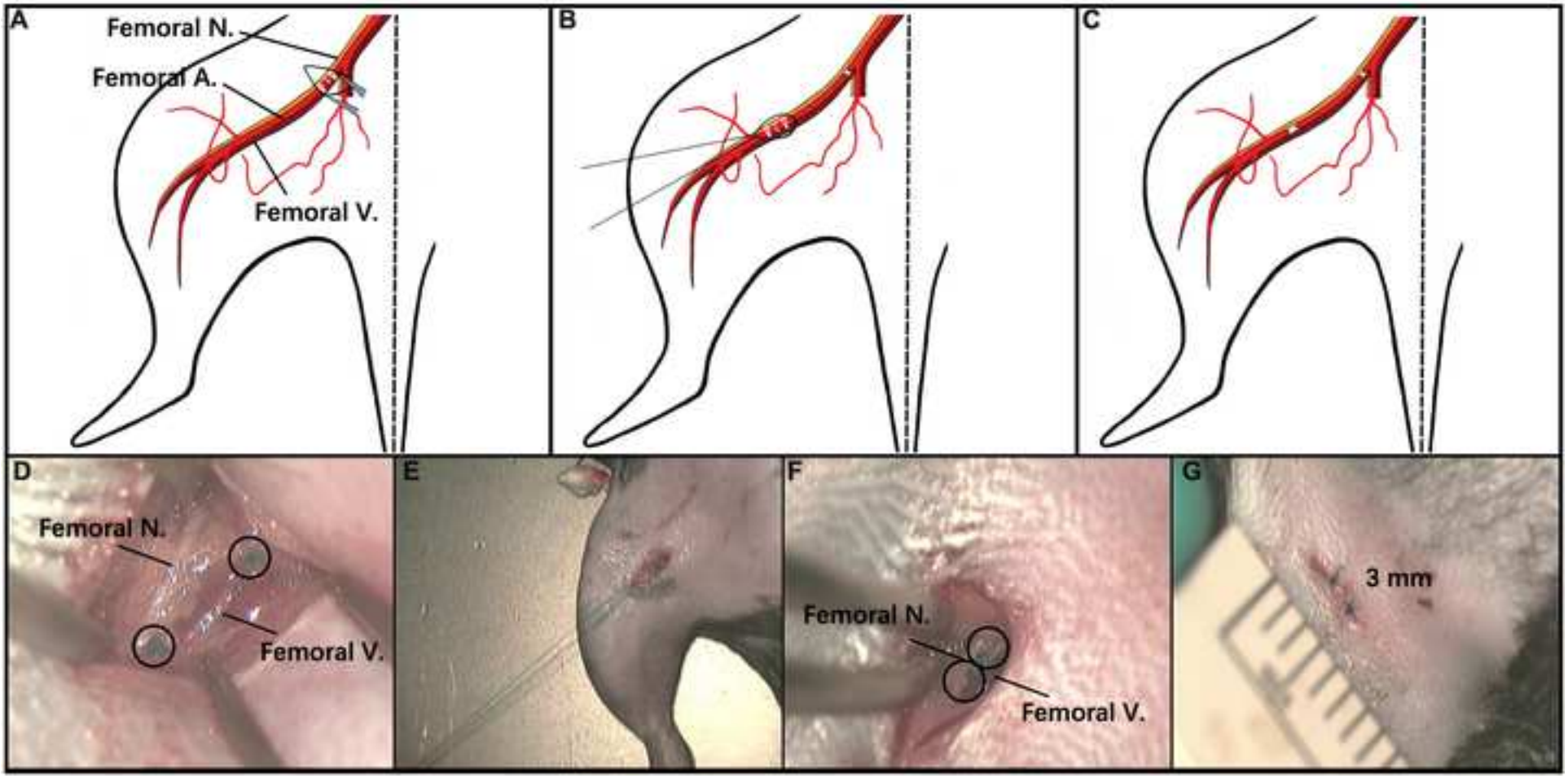

Figure-3

Click here to access/download;Figure;Figure 3 Characteristics of the PAD mice model.tiff

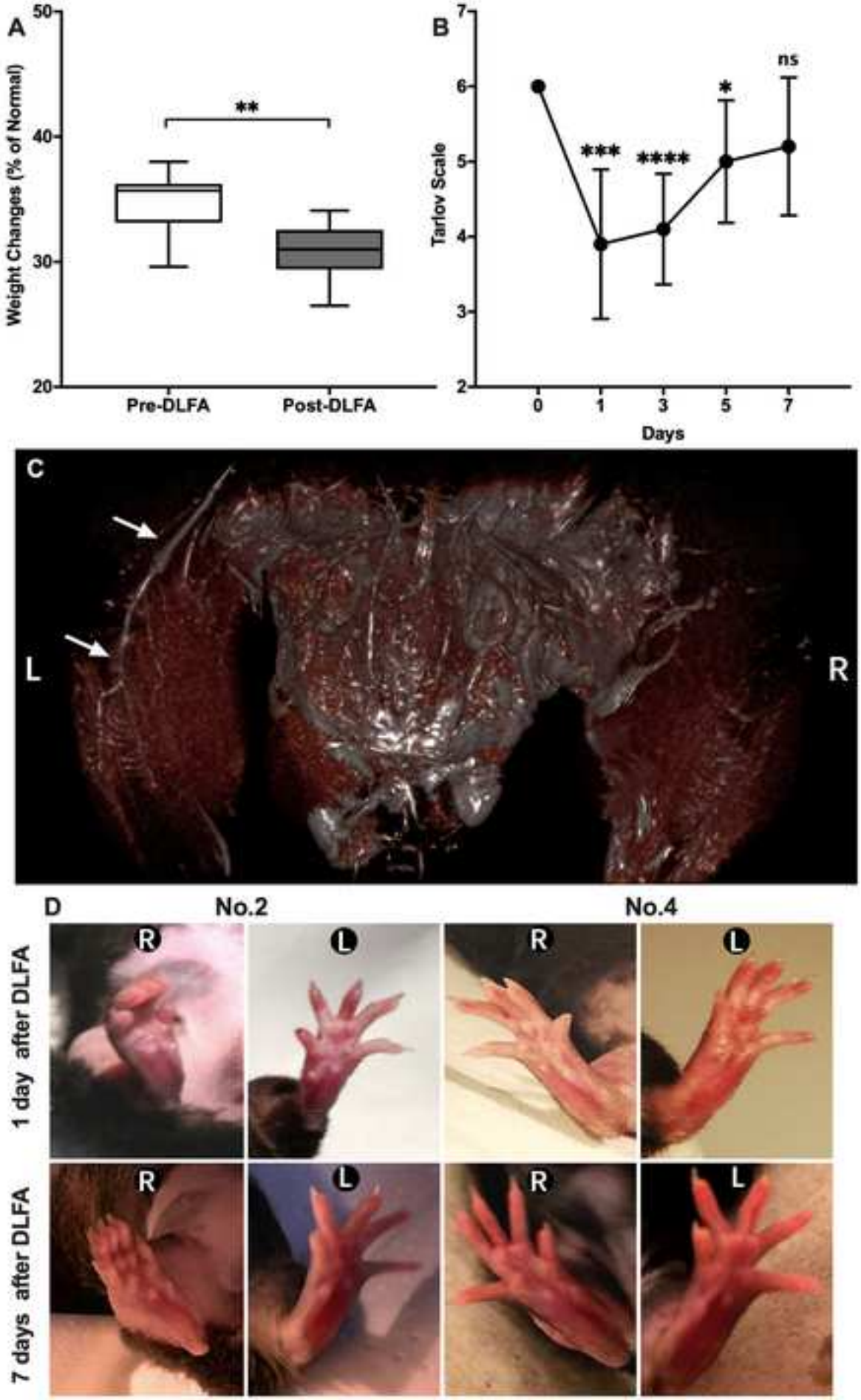

Figure-4

Click here to access/download;Figure;Figure 4-revision.tiff

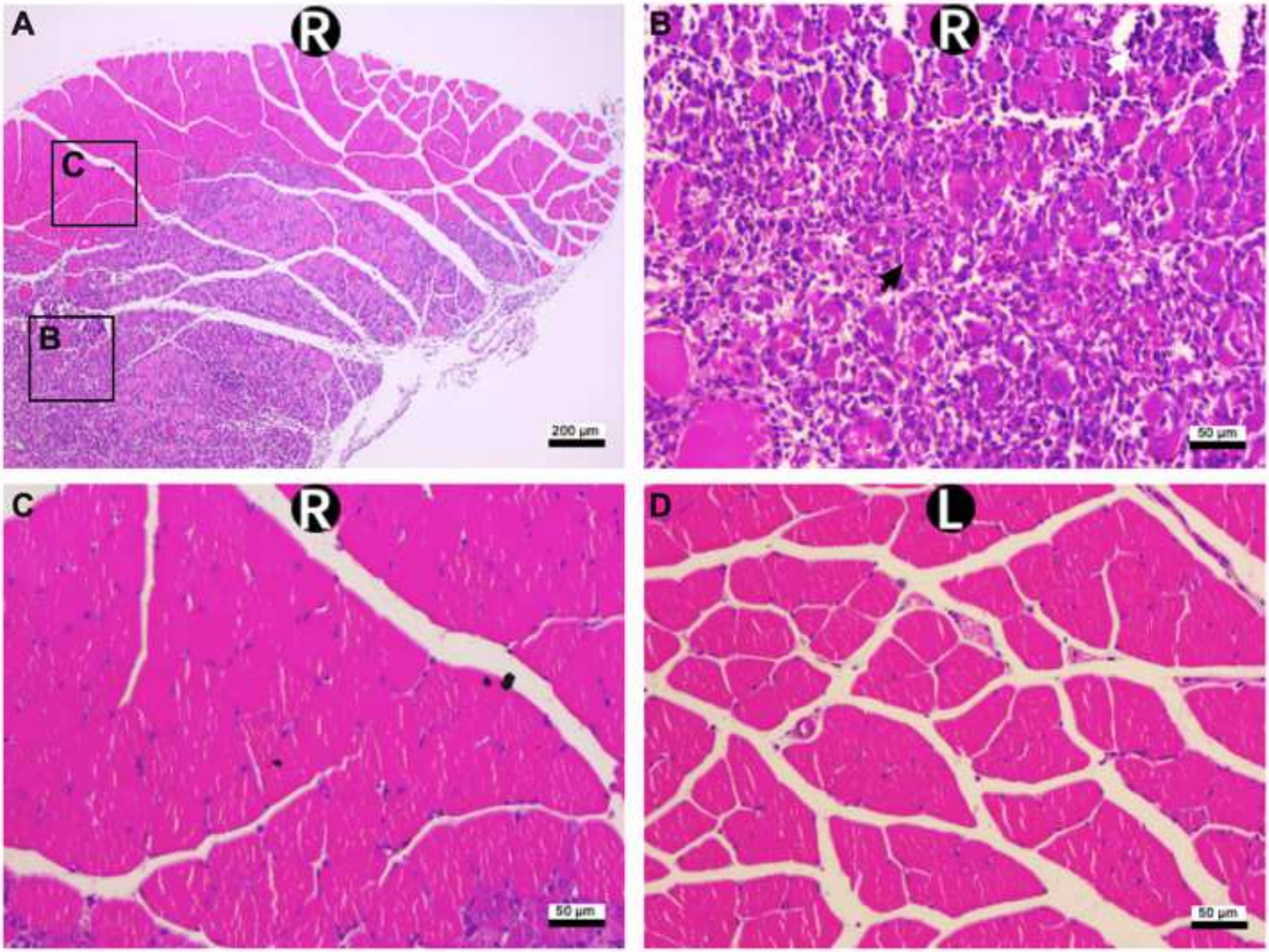

Figure-5

Click here to access/download;Figure;Figure 5-revision.tiff

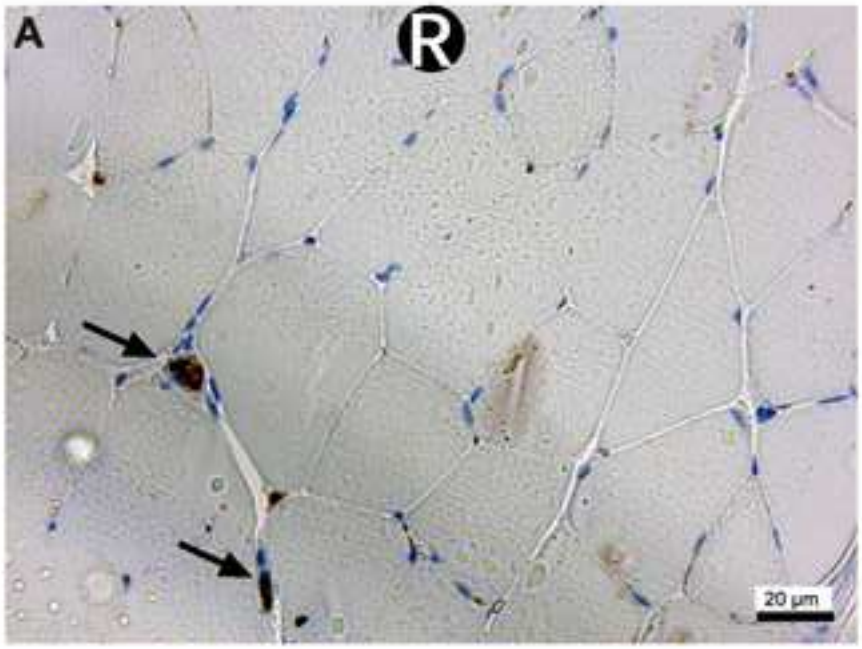

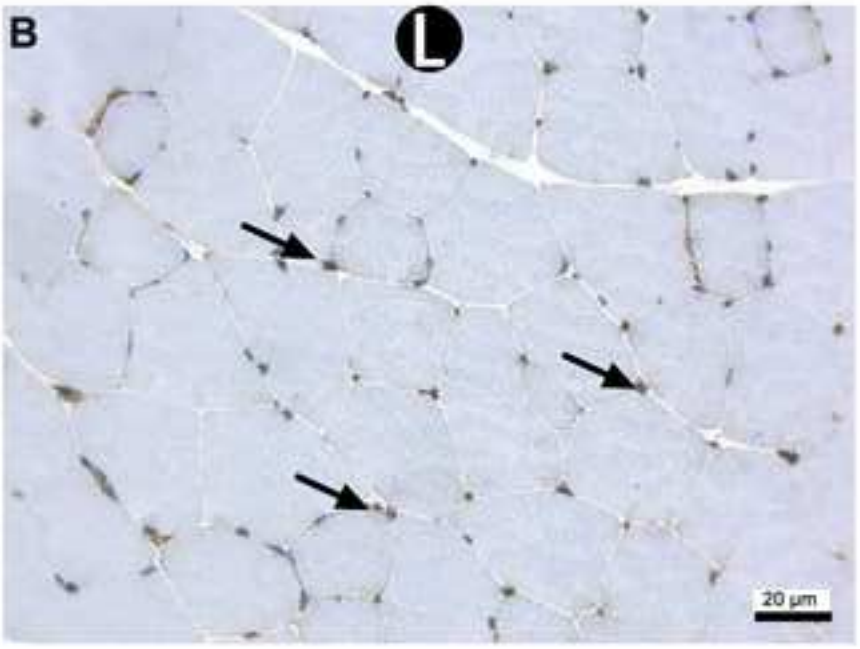

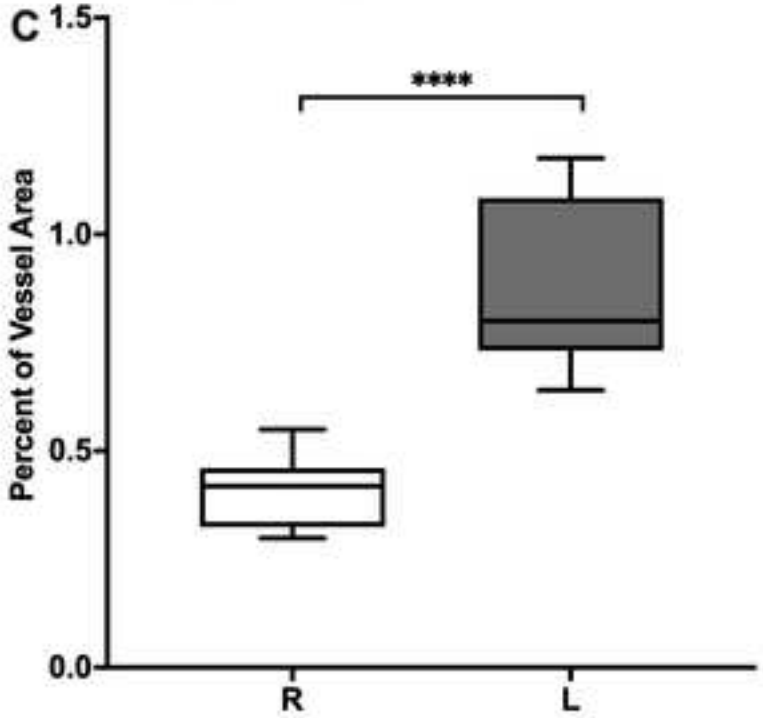

Table 1 Functional Scoring

Tarlov Score	0	No movement
	1	Barely perceptible movement, non-weight bearing
	2	Frequent movement, non-weight bearing
	3	Supports weight, partial weight bearing
	4	Walks with mild deficit
	5	Normal but slow walking
	6	Full and fast walking

Table of Materials

Click here to access/download;Table of Materials;TABLE OF MATERIALS_Revision.xls

Name of Material/ Equipment	Company	Catalog Number
10x Phosphate-buffered saline	Roth	9143.1
30% H_2O_2	Roth	9681.2
6-0 absorbable sutures	PROLENE	8776H
7-0 absorbable sutures	PROLENE	EH8021E
Acetic acid	Roth	6755.1
Albumin Fraktion V	Roth	8076.2
Axio vert A1 microscope	Carl Zeiss	ZEISS Axio Vert.A1
Bruker BioSpec 94/20 AVIII	Bruker Biospin MRI GmbH	N/A
CD31 antibody	Abcam	ab28364
Eosin Y solution 0.5% in water	Roth	X883.1
Epitope Retrieval Solution pH 6	Leica Biosystems	6046945
Ethanol ≥ 99.5%	Roth	5054.1
Fentanyl	Cayman Chemical	437-38-7
Fine point forceps	Medixplus	93-4505S
Graefe iris forceps curved	VUBU	VUBU-02-72207
Hair Remover	Veet	108972
Heating plate	STÖRK-TRONIC	7042092
Hematoxylin	Roth	T865.2
Leica surgical microscope	Leica	M651
Liquid DAB+Substrate Chromogen System	Dako	K3468
Male ApoE-/- mice	Charles River Laboratories	N/A
Medetomidine	Cayman Chemical	128366-50-7
Micro Needle Holder	Black & Black Surgical	B3B-18-8
Micro suture tying forceps	Life Saver Surgical Industries	PS-MSF-145
Microtome	Biobase	Bk-Mt268m
Midazolam	Ratiopharm	44856.01.00
MR-compatible Small Animal Monitoring and C	SA Instruments	N/a
Ointment for the eyes and nose	Bayer AG	1578675
Paraformaldehyde	Roth	0335.1
Pentobarbital	Nembutal	76-74-4
Paint brush	Marabu	1920000002
Saline	DeltaSelect	1299.99.99
Spring handle scissors with fine, sharp tips	Black & Black Surgical	B66167
SuperCut Scissors	Black & Black Surgical	B55992
Triton X-100	Roth	9002-93-1
Western diet, 1.25% Cholesterol	ssniff Spezialdiäten GmbH	E15723-34
Xylene	Roth	4436.3

Comments/Description

Used for hematoxylin and eosin stain and immunohistochemistry stain

Used for immunohistochemistry stain
Used for stitching the skin
Used for ligating the artery
Used for hematoxylin and eosin stain
Used for immunohistochemistry stain

Used for viewing and taking the pictures from hematoxylin and eosin stain and immunohistochemistry stain
Scan the femoral artery blockage
Used for immunohistochemistry stain
Used for hematoxylin and eosin stain
Used for immunohistochemistry stain
Used for hematoxylin and eosin stain and immunohistochemistry stain
Used for anesthesia
Used for separating the artery from nerve and vein
Used for blunt separation of skin and subcutaneous tissue
Remove hair from mouse hind limbs
Keep the stable temperature of mice
Used for hematoxylin and eosin stain and immunohistochemistry stain
Enlarge the field of view to facilitate the operation
Used for immunohistochemistry stain
Used for establish the Peripheral artery disease mice model
Used for anesthesia
Holding the needle
Used to assist in knotting during surgery
Used for tissue sectioning
Used for anesthesia
monitoring vital signs of animal during MRI scan
Keep the eyes wet under the anesthesia
Used for fixation of the tissue
Used for anesthesia
Used for picking up cut tissue section
Used for anesthesia

Used for cutting the artery
Used for cutting the skin
Used for immunohistochemistry stain

Used for hematoxylin and eosin stain and immunohistochemistry stain

UMM
UNIVERSITÄTSMEDIZIN
MANNHEIM

Medizinische Fakultät Mannheim
der Universität Heidelberg
Universitätsklinikum Mannheim

Haus 37, Station 37-4
Department of Surgery,
Medical Faculty Mannheim,
Heidelberg University
Mannheim, Germany
Theodor-Kutzer-Ufer 1-3
68161 Mannheim, Germany
Telefon: +49 621 383-1501
Telefax: +49 621 383-2166

To
Editorial team
JOVE
14 April 2021

Rebuttal letter: Manuscript number JoVE62402

Dear Editor,

We sincerely thank you and all reviewers for the feedback on our manuscript entitled "A novel surgical model of hind limb ischemia in ApoE$^{-/-}$ mice" (Manuscript number- JoVE62402). We found the comments from editorial members and reviewers very helpful in improving the manuscript.

In the following, we have addressed the comments/questions in a point-by-point manner where reviewers comments are formatted in ***italic and bold*** and our replies are formatted in simple text.

We hope the revised manuscript will find your approval for publication in JOVE.

On behalf of all authors

Sincerely yours,

Michael Keese

Rebuttal letter: Manuscript number JoVE62402

A novel surgical model of hind limb ischemia in ApoE$^{-/-}$ mice

Editorial comments:

1. ***Please take this opportunity to thoroughly proofread the manuscript to ensure that there are no spelling or grammar issues.***

   Response: Authors thank the editorial team for this suggestion and have carefully proofread the manuscript and resolved all the spelling and grammar issues.

2. ***Please take this opportunity to go through the edited version of your manuscript (62402_R1_edited) to address the editorial comments inserted in different places in the text.***

   Response: Authors agree with the all editorial comments and have implemented the changes as requested. Appropriate, response is also appended in the manuscript.

3. ***After going through the reviewers' comments, please make all changes to this edited document with track changes on, retaining the formatting style and other style changes made to meet JoVE's style.***

   Response: Authors have made changed in the document in the Microsoft Word track changed mode.

4. ***Being a video based journal, JoVE authors must be very specific when it comes to the humane treatment of animals. Regarding animal treatment in the protocol, please add the following information to the text, please specify the use of on eyes to prevent dryness while under anesthesia.***

   Response: Authors guarantee that animals have been treated humanely during the execution of the experiments and have added the missing information regarding the use of vet ointment (01578675, Bayer AG, Germany) on the eyes of mice while animals were under anesthesia in the manuscript.

5. ***Line 157: What do you mean by "mount the section on a charge slide"?***

   Response: Authors have modified the text to make it clear and easy to understand.

6. ***Please add a space between the number and units in Figure 2 and just use the numbers in Figure 3 (instead of 0th, 1st etc).***

   Response: The space was added between the number and units in Figure 2 and corresponding correction has been made in Figure 3.

7. ***Please consider attaching Table 2 (summary of the 25 most recent …) as a supplementary file.***

   Response: As advised, authors, provide Table 2 (Summary of the current 25 literature to establish PAD model) as supplementary file.

8. ***Please revise the following lines to avoid overlap with previously published work: 156-157; 172-174; 180-181; 195-198; 204***

   Response: Authors have revised the manuscript to avoid overlap with previously published work.

Reviewer #2:

I am delighted to review the manuscript entitled "A novel surgical model of hind limb ischemia in ApoE$^{-/-}$ mice". The manuscript is generally well written but I have a few major concerns

Major Concerns:

"Second, several mouse strains, such as immune deficient mice including severe combined immunodeficiency or nude mice, are very fragile, and large incisions, as well as additional anesthesia, may result in death". Inaccurate statement it's not the length of the incision but the severity of the inflicted ischemia. (Paronis et al 2020). Discussion had greatly changed but it's still not convincing.

Response: We agree and have revised accordingly. The evidence cannot support that smaller incision lead to less anesthesia application. The related content is corrected, and the part is deleted.

Minor Concerns:

Please try to mention your findings in the discussion. The authors had done enough work and it should be discussed in the discussion section.

Response: The author welcomes comments from reviewer and have modified the discussion to address the main findings. To this end we discuss our main findings and relate them to clinical characteristic of the PAD patients - the histological and functional results are also discussed to show their relevance to peripheral arterial disease. Furthermore, we also discussed the advantages of this modification method and the reasons for choosing it. The reasons for using ApoE$^{-/-}$ mice are also discussed. Finally, we discussed the limitations of these methods.

***Reviewer #3**:*

The authors have addressed the concerns raised in the first review.

Response: Authors thank the reviewer number 3 for the comment.

Editorial Office,

JOVE,

14th December. 2020

Dear Editor,

We would like to submit our **article**, "**An improved model of hind limb ischemia in ApoE-/- mice**", for consideration for publication in **JOVE**.

Preclinical hindlimb ischemia animal models are usually generated through double ligations of the femoral artery (DLFA). However, this approach usually needs a relatively large incision thus increasing trauma to the animals. Here we describe an alternative approach with a very small invasion without any necessary hardware upgrade in the lab.

This article has not been submitted elsewhere. All authors have read and approved the content of this manuscript and agree with its submission to this journal for publication. There are no ethical/legal conflicts associated with the publication of this article.

Your consideration of this manuscript is greatly appreciated.

With kind regards,

Michael Keese

E-mail: Michael.keese@umm.de

No.	Year	Literature	Journal	Mouse type	Occlusion artery	Incision place	Size (cm)
1	2008	A Quantitative Trait Locus (LSq-1) on Mouse Chromosome 7 Is Linked to the Absence of Tissue Loss After Surgical Hindlimb Ischemia	Circulation	C57BL/6 mice	Femoral artery	Inguinal region	N/G
2	2009	Murine model of hindlimb ischemia	J Vis Exp	N/G	Proximal and distal femoral artery	From the knee towards the medial thigh	1
3	2009	A functional murine model of hindlimb demand ischemia	Ann Vasc Surg	ApoE$^{-/-}$ mice	The femoral artery and visible branches	Longitudinally on the anterior thigh of the left hind limb	0.5–1
4	2010	A new murine model of sustainable and durable chronic critical limb ischemia fairly mimicking human pathology	Eur J Vasc Endovasc Surg	Swiss mice	Iliac artery, femoral artery, superficial epigastric artery, popliteal and saphenous arteries	From the knee towards the abdomen	N/G
5	2010	Variations in surgical procedures for hind limb ischaemia mouse models result in differences in collateral formation	Eur J Vasc Endovasc Surg	C57BL/6 mice	Femoral artery including all superficial and deep branches	Inguinal region till the knee	N/G
6	2011	Supramolecular nanostructures that mimic VEGF as a strategy for ischemic tissue repair	Proc Natl Acad Sci U S A	FVB mice	Femoral artery including all superficial and deep branches	From the knee towards the abdomen	N/G
7	2011	NADPH oxidase 4 promotes endothelial angiogenesis through endothelial nitric oxide synthase activation	Circulation	C57BL/6 mice	Proximal and distal femoral artery	Nguinal region	1.5-2
8	2012	Toward a mouse model of hind limb ischemia to test therapeutic angiogenesis	J Vasc Surg	C57BL/6 mice	High femoral artery and superficial femoral artery	From the knee towards the abdomen	N/G
9	2012	Endothelial progenitor cell· derived microvesicles improve neovascularization in a murine model of hindlimb ischemia	Int J Immunopathol Pharmacol	C57BL/6 mice	Femoral artery and saphenous artery	Inguinal region till the knee	N/G

10	2013	MicroRNA-93 controls perfusion recovery after hindlimb ischemia by modulating expression of multiple genes in the cell cycle pathway	Circulation	C57BL/6 mice	Femoral artery	Inguinal region	N/G
11	2013	Limb ischemia after iliac ligation in aged mice stimulates angiogenesis without arteriogenesis	Nanoscale	C57BL/6 mice	Iliac artery and iliac vein	Abdomen	0.5–1
12	2013	mTORC1 and mTORC2 Play Different Roles in the Functional Survival of Transplanted Adipose-Derived Stromal Cells in Hind Limb Ischemic Mice Via Regulating Inflammation In Vivo	Stem Cells	C57BL/6 mice	Femoral artery including all superficial and deep branches	Inguinal region till the knee	N/G
13	2013	Hydrogen molecules (H2) improve perfusion recovery via antioxidant effects in experimental peripheral arterial disease	Mol Med Rep	Balb/c mice	Femoral artery	Inguinal region	N/G
14	2014	Experimental peripheral arterial disease: new insights into muscle glucose uptake, macrophage, and T-cell polarization during early and late stages	Physiol Rep	ApoE$^{-/-}$ mice	Iliac artery above internal–external iliac artery bifurcation, epigastric artery and saphena and popliteal arteries	Abdominal incision	N/G
15	2015	VEGF-loaded graphene oxide as theranostics for multi-modality imaging-monitored targeting therapeutic angiogenesis of ischemic muscle	Nanoscale	N/G	Femoral artery	From the knee towards the abdomen	N/G
16	2016	Methods for Acute and Subacute Murine Hindlimb Ischemia	J Vis Exp	N/G	Proximal and distal femoral artery	From the knee towards the abdomen	1
17	2017	CD34+/M-cadherin+ Bone Marrow Progenitor Cells Promote Arteriogenesis in Ischemic Hindlimbs of ApoE2/2 Mice	PLoS ONE	ApoE$^{-/-}$ mice	Proximal left femoral artery and vein	Inguinal region	N/G

18	2017	Serum-derived extracellular vesicles (EVs) impact on vascular remodeling and prevent muscle damage in acute hind limb ischemia.	Sci Rep	C57BL/6 mice	Femoral artery and saphenous artery	Inguinal region till the knee	N/G
19	2018	Acute and chronic effects of exercise on mRNA expression in the skeletal muscle of two mouse models of peripheral artery disease	PLoS One	C57BL/6 mice	Proximal and distal ends of the femoral artery and the proximal profunda femoris artery	From the knee towards the abdomen	N/G
20	2018	A Murine Model of Hind Limb Ischemia to Study Angiogenesis and Arteriogenesis	Methods Mol Biol	N/G	Femoral/saphenous artery	From ~7 mm below the inguinal region and ~3 mm	1
21	2019	Pretreatment of Diabetic Adipose-derived Stem Cells with mitoTEMPO Reverses their Defective Proangiogenic Function in Diabetic Mice with Critical Limb Ischemia	Cell Transplant	C57 mice	Femoral artery including all superficial and deep branches	Inguinal region till the knee	N/G
22	2019	Treating ischemia via recruitment of antigen-specific T cells	Sci Adv	B6.Cg-Tg(TcraTcrb)425bn/J or BALB/c mice	External iliac and femoral artery and vein ligation	Nguinal region	N/G
23	2019	Extracellular Vesicles From Adipose Stem Cells Prevent Muscle Damage and Inflammation in a Mouse Model of Hind Limb Ischemia: Role of Neuregulin-1	Arterioscler Thromb Vasc Biol	C57BL/6 mice	Femoral artery and saphenous artery	Inguinal region till the knee	N/G
24	2019	Hyperglycaemia and Ischaemia Impair Wound Healing via Toll-like Receptor 4 Pathway Activation in vitro and in an Experimental Murine Model.	Eur J Vasc Endovasc Surg	C57BL-6 or TLR4 knockout mice	External iliac artery and ligation-excision of the superficial femoral artery	Inguinal region	N/G

25	2019	Neural JNK3 regulates blood flow recovery after hindlimb ischemia in mice via an Egr1/Creb1 axis.	Nat Commun	C57BL/6 mice	Proximal and distal femoral artery	Inguinal region	1.5-2

G: Not Given